High resolution emission Fourier transform infrared spectra of the 4 p - 5 s and 5 p - 6 s bands of ArH

O. I. Baskakov, S. Civiš, and K. Kawaguchi

Citation: The Journal of Chemical Physics **122**, 114314 (2005); doi: 10.1063/1.1862622
View online: http://dx.doi.org/10.1063/1.1862622
View Table of Contents: http://scitation.aip.org/content/aip/journal/jcp/122/11?ver=pdfcov
Published by the AIP Publishing

High resolution emission Fourier transform infrared spectra of the 4*p*-5*s* and 5*p*-6*s* bands of ArH

O. I. Baskakov
Faculty of Quantum Radiophysics, Kharkov National University, Svobody square 4, 61077 Kharkov, Ukraine

S. Civiš[a)]
J. Heyrovský Institute of Physical Chemistry, Academy of Sciences of the Czech Republic, Dolejškova 3, 182 23 Praha 8, Czech Republic

K. Kawaguchi
Department of Chemistry, Faculty of Science, Okayama University, Tsushima-naka 3-1-1, Okayama 700-8530, Japan

(Received 1 November 2004; accepted 7 January 2005; published online 23 March 2005)

In the 2500–8500 cm^{-1} region several strong emission bands of ^{40}ArH were observed by Fourier transform spectroscopy through a dc glow discharge in a mixture of argon and hydrogen. Rotational-electronic transitions of the two previously unstudied 4*p*-5*s* and 5*p*-6*s*, $v=0$-0, bands of ^{40}ArH were measured and assigned in the 6060 and 3770 cm^{-1} regions, respectively. A simultaneous fit of the emission transitions of the 4*p*-5*s* and 5*p*-6*s* bands and an extended set of transitions of the 6*s*-4*p* band observed by Dabrowski, Tokaryk, and Watson [J. Mol. Spectrosc. **189**, 95 (1998)] and remeasured in the present work yielded consistent values of the spectroscopic parameters of the electronic states under investigation. In the branch of the 4*p*-5*s* band with transitions of type $^{Q}Q_{f_{3}e}$ we observed a narrowing in the linewidths with increasing rotational quantum number *N*. The rotational dependence of the linewidth is caused by predissociation of the 5*s* state by the repulsive ground 4*s* state through homogeneous coupling and changes in overlap integrals of the vibrational wave functions with the rotational level. Analysis was based on the Fermi's golden rule approximation model. In the 4*p*-5*s* band region a vibrational sequence of v'-v''=1-1, 2-2, and 3-3 were recorded and a number of transitions belonging to the strongest $^{Q}Q_{f_{3}e}$ form branch of the 1-1 band were analyzed. © *2005 American Institute of Physics*.
[DOI: 10.1063/1.1862622]

I. INTRODUCTION

ArH is representative of the rare gas monohydrides that are unstable in their repulsive ground states but stable in their bound Rydberg states. These properties of the rare gas hydrides were predicted by *ab initio* calculations, beginning with the work of Michels and Harris on HeH in the early 1960s,[1] and were confirmed in numerous experimental studies from HeH to XeH.

ArH was the first member of the rare gas hydrides for which an emission spectrum was obtained in pioneering work by Johns.[2] The observed spectrum consisted of a relatively simple band near 13 040 cm^{-1}, and detailed rotational analysis showed that the spectrum is due to a $^2\Pi$-$^2\Sigma$ transition in a Hund's case (b) limit. The succeeding study on ArH (Ref. 3) was reported nearly 20 years after the first one, despite several attempts to analyze another observed band near 6100 cm^{-1} undertaken in 1980 and again in 1983.[4] The most extensive spectroscopic studies have been performed over the past decade [4–8] at the National Research Council of Canada. Since ArH is short lived and unstable, the authors used special techniques to produce this species in the bound excited electronic states. As a result of this work, many bands have been analyzed and the structures of the lower electronic excited states are understood. Many electronic states are strongly coupled to form Rydberg complexes, so the *nl* notation in the limit of a united atom is used for the state category.[5] It was also found that the rotational levels of the lowest bound 5*s*($A\,^2\Sigma^+$) state are predissociated by interaction with the repulsive $X\,^2\Sigma^+$ state.

It should be noted that ArH has always been studied together with its deuterated species ArD, which is more stable and for which the spectra are stronger. The rotational constant of ArD is about half of that for ArH, so the range of rotational quantum numbers in the spectra taken at the same T_{rot} is wider, the rotational levels are less perturbed by the neighboring vibrational-electronic states, and the predissociation rate of the 5*s* state is lower than that of ArH. For example, the linewidth of the $3d\pi \rightarrow 5s$ transition in ArH is reported to be about 1 cm^{-1}, whereas the linewidth in ArD is much narrower, about 0.03 cm^{-1}.[2] As a consequence electronic bands of ArD have been studied more extensively than the respective bands of ArH. All observed and identified bands are listed in Table I.

The present paper reports rotational analysis of the

[a)]Author to whom correspondence should be addressed. Electronic mail: civis@jh-inst.cas.cz

TABLE I. Investigated bands of ArH and ArD.

Transition	ArH Band origin (cm^{-1})	ArD Band origin (cm^{-1})	Resolution (cm^{-1})	Reference
$3d\pi \rightarrow 5s$	13 024	13 040	0.1	2
$4d\pi \rightarrow 5s$	19 520	19 570		3
$\pi \rightarrow 5s$?	⋯	22 575		3
$5p \rightarrow 5s$	⋯	17 487	0.13	5
$5p \rightarrow 6s$	⋯	3 681	0.20	5
$6p \rightarrow 5s$	⋯	21 676	0.20	5
$4p \rightarrow 5s$	⋯	6 120	0.05;0.2	4
$3d\sigma \rightarrow 4p$	⋯	10 200	0.05;0.2	4
$3d\pi \rightarrow 4p$	6 934	6 900	0.05;0.2	4,6
$3d\delta \rightarrow 4p$	8 534	8 524	0.05	6
$4d\sigma \rightarrow 4p$	15 097	15 075	0.3	6
$6s \rightarrow 4p$	7 703	7 685	0.02	6
$8s \rightarrow 4p$	⋯	16 749	0.20	6
$4f \rightarrow 5s$	20 641	20 682	0.20	7
$4f \rightarrow 3d\pi$	7 627	7 649	0.05	7
$4f \rightarrow 3d\delta$	6 027	6 038	0.05	7
$4f \rightarrow 3d\sigma$	~4 400	4 351	0.10;0.20	7,8

$4p$-$5s$ and $5p$-$6s$ $v=0$-0 bands centered at 6060 and 3770 cm^{-1}. To derive a consistent set of spectroscopic parameters of the $5s$, $4p$, $6s$, and $5p$ states, the $6s$-$4p$ band initially recorded by Dabrowski, Tokaryk, and Watson[6] has been remeasured and extended, and rotational structures of these three bands were fitted simultaneously. Additionally, the rotational lines of ArH originating from the $v=1$-1 band of the $4p$-$5s$ transition have been assigned.

II. EXPERIMENTAL DETAILS

As was pointed out by Johns,[2] spectra of ArH and ArD can be observed in almost any form of electrical discharge through mixtures of argon and hydrogen or deuterium. In previous studies spectra have been observed using different sources: a Penning ionization cell (Cossart tube),[3–6,8] a Corona-discharge jet source,[4–7] and a sealed lamp.[2]

In the present study, ArH was generated in a dc glow discharge in a gas mixture of Ar and H_2 inside a glass cell of 25 cm in length and 1 cm in diameter. The optimum conditions were found to be about 4.3 Torr of Ar and 400 mTorr of H_2. The dc discharge current could be changed from 100 to 500 mA and a smooth increase of emission intensity with current was found. The spectra with a resolution of 0.055 cm^{-1} were collected with a Bruker IFS 120HR Fourier transform spectrometer equipped with a liquid-nitrogen-cooled InSb detector. In total 1000 scans were coadded and a S/N ratio of 40 was obtained for the strongest lines of the $5p$-$6s$ band. Wave number calibration was provided by Ar atomic lines. The uncertainty in the measured strong unblended line positions is estimated to be one-tenth of the resolution of about ± 0.005 cm^{-1}.

III. EFFECTIVE HAMILTONIAN

The authors of the previous studies[5–8] treated the electronic states of ArH as the levels of so-called l complexes. The l complex is a group of levels with equal values of the principal and orbital quantum numbers n and l. In the first of these papers[5] the effective Hamiltonian describing spin-rotation energy level structure of the states with definite l value has been developed and successfully used in the following papers. However, as a rule, electronic orbital momentum l is not a good quantum number since momentum is not a conserved quantity in a molecule. It is difficult to use the l-complex Hamiltonian to account for interactions between the vibronic states, which do not belong to the same l complex. Therefore we used a more general form of Hamiltonian which was similar to that described by Zare *et al.*[9] and Brown *et al.*[10] Generally, it may be represented as a sum of the following terms:

$$\left\{\tfrac{1}{2}[N^{2i},(\hat{L}_{mn}\hat{S}_{pr}\hat{J}_{tq}+\hat{L}_{m-n}\hat{S}_{p-r}\hat{J}_{t-q})]_+\right\}_{v,w}, \tag{1}$$

where $[X,Y]_+=XY+YX$. Outer subscripts v and w denote whether the term concerns a given electronic-vibrational state ($v=w$) or couples two different states ($v\neq w$). $\hat{L}_{mn},\hat{S}_{pr},\hat{J}_{tq}$ operators are determined by the expression

$$\hat{\mathbf{G}}_{ik}=\tfrac{1}{2}[\mathbf{G}_z^i\mathbf{G}_\pm^{|k|}+\mathbf{G}_\pm^{|k|}\mathbf{G}_z^i], \tag{2}$$

where $\mathbf{G}$ stands for one of the L, S, or J operator, and $\mathbf{G}_\pm=\mathbf{G}_x\pm i\mathbf{G}_y$ are the angular momentum ladder operators. The z axis is chosen to lie along the internuclear axis. The subscript i in this expression is a positive integer while k can be both positive and negative. If k is greater than 0, then this expression will be

$$\hat{\mathbf{G}}_{ik}=\tfrac{1}{2}[\mathbf{G}_z^i\mathbf{G}_+^{|k|}+\mathbf{G}_+^{|k|}\mathbf{G}_z^i].$$

If k is negative, then it will be

$$\hat{\mathbf{G}}_{ik}=\tfrac{1}{2}[\mathbf{G}_z^i\mathbf{G}_-^{|k|}+\mathbf{G}_-^{|k|}\mathbf{G}_z^i].$$

N^2 in Eq. (1) (square of the rotational angular momentum) is determined by

$$N^2=(\vec{J}-\vec{S})^2. \tag{3}$$

The effective Hamiltonian (1) consists of an infinite number of terms.[9,10] Every term is expressed with various factors of angular momentum operators. This Hamiltonian should to be Hermitian and invariant under symmetry operations and time reversal. In the phenomenological theory of diatomic molecules there are five angular momenta (excluding nuclear spin): J (total), L (electronic orbital), S (electronic spin), R (rotational), and N (total mechanical). Only three of them are independent. The molecule-fixed components of J, L, and S have been used, since they all commute, and N^2 as an invariant operator. The commutation properties of the chosen operators significantly facilitate evaluation of the Hamiltonian matrix elements. Furthermore, the terms may be divided into two groups: those which relate to a specific electronic vibrational states and form diagonal blocks of the Hamiltonian matrix and those which determine an interaction between two states and contribute to off-diagonal blocks. There are no terms which have matrix elements both in diagonal and off-diagonal blocks.

In expression (1) n must be $\geqslant 0$, r may be an arbitrary integer, and n, r, and q must satisfy the equality $n+r+q=0$ because of the relation $J_z=L_z+S_z$. The powers of the $L_\pm$ ladder operators can only be equal to the differences of Λ, eigenvalues of L_z, of interacting electronic vibrational states, and 0 or 2Λ for a given vibronic state.

This expression gives a general form of any term of the Hamiltonian. The low order terms are the principal terms. For example, the term with $i=1, m=n=p=r=t=q=0 (v=w)$ corresponds to a pure rigid rotation of a molecule, and the term having $i=n=r=t=q=0, m=p=1 (v=w)$ represents parallel spin-orbital interaction. The magnitude of the terms decreases as a total power of the term increases. Higher order terms describe centrifugal distortion effects and the influence of other electronic states. They appear in different orders of the perturbation theory.

To build a matrix of the Hamiltonian the unsymmetrized case (a) basis set is used

$$|n,v,\Lambda,J,\Omega=\Lambda+\Sigma,S,\Sigma\rangle. \tag{4}$$

These functions are common eigenfunctions of the electronic Hamiltonian of nonrotating molecule,[11] vibrational Hamiltonian, and the operators J^2, S^2, J_z, S_z, and L_z with eigenvalues ε_n, ε_v, $J(J+1)$, $S(S+1)$, Ω, Σ, and Λ, respectively, but the L^2 operator is not diagonal in this representation. n and v denote the electronic and vibrational states. The phase convention is chosen in such a way that matrix elements of $S_\pm$ and $J_\pm$ have the form

$$\langle J,\Omega|J_\pm|J,\Omega\pm1\rangle=\sqrt{J(J+1)-\Omega(\Omega\pm1)},$$

$$\langle S,\Sigma|S_\pm|S,\Sigma\mp1\rangle=\sqrt{S(S+1)-\Sigma(\Sigma\mp1)}. \tag{5}$$

The diagonal blocks of the effective Hamiltonian have diagonal matrix elements in n, v, J, and S quantum numbers. For the vibronic states of interest in the present study, $^2\Sigma$ and $^2\Pi$, the diagonal blocks can be written as

$$\begin{aligned}H_{ii}=&T_i+B_iN^2-D_iN^4+H_iN^6+L_iN^8,\\&+\frac{1}{2}\left[\left(\frac{A_i^{\|}}{2}\right)+\left(\frac{A_{Di}^{\|}}{2}\right)N^2+\left(\frac{A_{Hi}^{\|}}{2}\right)N^4,2L_zS_z\right]_+\\&+\frac{1}{2}\left[\left(\frac{\gamma_i}{2}\right)+\left(\frac{\gamma_{Di}}{2}\right)N^2,(S_+J_-+S_-J_+)\right]_+\left(\frac{p_i}{2}\right)\\&\times(\overline{L_+^2}S_-J_-+\overline{L_-^2}S_+J_+),\end{aligned} \tag{6}$$

where only the terms determined in a least-squares fit are shown.

The last term of Eq. (6) denotes the effect of Λ doubling in $^2\Pi$ states. This term has been written in such a manner to emphasize that it connects the states with opposite signs $\Lambda=\pm1$. In Eq. (6) we have introduced an abbreviation for the matrix elements of L_+^2, L_-^2

$$\overline{L_\pm^2}=\langle n,\Lambda=+1|L_+^2|n,\Lambda=-1\rangle=\langle n,\Lambda=-1|L_-^2|n,\Lambda=+1\rangle, \tag{7}$$

and p_i is the Λ-type doubling parameter. In the calculation the parameter appears as $p_i\overline{L_+^2}=p_i\overline{L_-^2}$. In the case (d) basis set used by Watson, [6,7] l is a good quantum number and for Π states $\overline{L_+^2}=\overline{L_-^2}=l(l+1)=2$.

The Hamiltonian of the $^2\Sigma$ states, namely, $5s\sigma$, $6s\sigma$, $4p\sigma$, and $5p\sigma$, is also given by Eq. (6), without the term responsible for Λ-type doubling. For $4p\pi$ and $5p\pi$ states all terms in Eq. (6) are considered.

In the off-diagonal blocks of the Hamiltonian, which connect $4p\sigma$ and $4p\pi$, and $5p\sigma$ and $5p\pi$ states, the essential terms are

$$\begin{aligned}H_{ij}=&\frac{1}{2}\left[\left(\frac{A_{ij}^{\perp}}{2}\right)+\left(\frac{A_{Dij}^{\perp}}{2}\right)N^2,(\overline{L_+}S_-+\overline{L_-}S_+)\right]_+\\&+\frac{1}{2}\left[\left(\frac{\xi_{ij}}{2}\right)+\left(\frac{\xi_{Dij}}{2}\right)N^2+\left(\frac{\xi_{Hij}}{2}\right)N^4,(\overline{L_+}J_-+\overline{L_-}J_+)\right]_+.\end{aligned} \tag{8}$$

The spin-orbit and orbit-rotation constants derived in the fit and listed in Table IV are given in the form $A_{ij}^{\perp}\overline{L_+}=A_{ij}^{\perp}\overline{L_-}$ and $\xi_{ij}\overline{L_+}=\xi_{ij}\overline{L_-}$, where

$$\overline{L_\pm}=\langle n,\Lambda=1|L_+|n',\Lambda=0\rangle=\langle n,\Lambda=-1|L_-|n',\Lambda=0\rangle. \tag{9}$$

In the case (d) basis set, $\overline{L_+}=\overline{L_-}=\sqrt{l(l+1)}=\sqrt{2}$.

It should be noted that some terms of the Hamiltonian in the present work are given in a somewhat unusual form, since their appearances originate from the general expression (1). Representation (1) does not lead to a loss of generality, but only to the regrouping of terms. For example, the familiar expression for the spin-rotation interaction [9,10] can be written in the form

$$\gamma\vec{N}\vec{S}=\gamma\left[\underline{\tfrac{1}{2}(S_+J_-+S_-J_+)}+\underline{L_zS_z}-\underline{(S^2-S_z^2)}\right]. \tag{10}$$

The first underlined term coincides with the main part of the spin-rotation interaction in Eq. (6), the second one is absorbed by $A^{\|}L_zS_z$, whereas the third is a constant incorporated into T.

Also, it should be noted that the Hamiltonian used in the present work in the case of isolated l complexes is similar to

that given in Ref. 5. The formal difference is that the matrix elements of powers of $L_{\pm}$ operators in Ref. 5 are evaluated using eigenfunctions of L^2, L_z rather than the formulas (7) and (9), and the angular momentum of a core $\vec{R}=\vec{N}-\vec{L}$ is used instead of $\vec{N}$. The data processing was performed using both the Hamiltonian given by Eqs. (6) and (8), and the *l*-complex Hamiltonian. Both approaches yielded similar results in quality. Neverthless, the final results in the present work are given with the constants of the effective Hamiltonian (6) and (8).

IV. OBSERVED SPECTRUM AND ANALYSIS

A. 4*p*-5*s* Band

The 5*s* state is the first excited bound electronic state. It is strongly predissociated by interaction with the unstable repulsive ground state $X\,^2\Sigma^+$, so the observed linewidth of the rotationally resolved spectral lines of ArH is $\sim$1.0 cm^{-1} while in ArD it is much sharper, $\sim$0.03 cm^{-1}. [2–4] As can be seen from Table I, a number of the bands with the 5*s* lower level have been recorded and analyzed, mostly for ArD. Two constants, *B* and *D*, of this state have already been determined by Johns[2] from three dozen rotational lines of the $3d\pi \rightarrow 5s$ band with a maximum $N=23$ and then used without refining in the following study,[3] where rotational transitions had smaller *N* values. Later Dabrowski, Tokaryk, and Watson[6] included these transitions in a simultaneous least-squares fit of the several bands related to the 5*s* state of ArH and obtained a somewhat improved set of the parameters for the state. At the same time they analyzed the ArD data to determine not only rotational and quartic centrifugal distortion constants but also the spin-rotation constant γ.

As was mentioned previously,[4] the 4*p*-5*s* band was observed around 6100 cm^{-1} several times by various methods both at low and high resolution. In all cases, the ArH spectrum appeared with much weaker intensity and a much less complete spectral pattern than the ArD one. For these reasons, and because this band of ArH was nearly unresolved, it seemed to be impossible to carry out a complete rotational analysis, whereas the rotational structure of the 4*p*-5*s* band of ArD has been analyzed and described in detail by Dabrowski *et al.*[4] The band appears to be very compact and it consists of *Q* form branches only. All ten allowed *Q* form branches characteristic for the *ns*-*n*′*p* transition were analyzed in the spectra of ArD.

In the present study we were able to distinguish about 100 $v=0$-0 rotational transitions in the recorded 4*p*-5*s* emission band of ArH having maximum value of $N'=35$. To identify the observed rotational structure it was supposed that selection rules and intensities for the ArH bands resemble those for ArD. An overview spectrum of the 4*p*-5*s* band is shown in Fig. 1. The sharp spectral lines are due to the 4*f*-3*d*δ transitions.[7] The central peak degraded to the low-frequency side is formed by a ${}^{Q}Q_{f_3e}$ form branch, and ${}^{Q}Q_{e_2f}$ form branch lines appear together with ${}^{Q}Q_{f_3e}$ on the lower frequency side. The high-frequency side wing is explained by the ${}^{Q}R_{f_2f}$- and ${}^{Q}R_{e_3e}$ form branches.

The assignment was made by a straightforward calculation of the rotational wave numbers using available parameters of the 4*s* and 5*p* states taken from Refs. 2 and 6. Because of the insufficient accuracy of constants derived from the analysis of transitions with low *N* values, there was an uncertainty of ± 1 in the quantum number *N* for the observed lines. This uncertainty was then removed by making a comparison between the calculated and observed line spacing in the allowed *Q* form branches. The wave numbers of assigned transitions are listed in Table II and the parameters derived are given in Tables III and IV. Despite the low accuracy of the measured wave numbers in the 4*p*-5*s* band, we could determine not only rotational and quartic centrifugal distortion parameters for the 5*s* state, but also sextic centrifugal distortion and two spin-rotational constants. It should be noted that the listed constants have been determined through the simultaneous fit of the 4*p*-5*s*, 5*p*-6*s*, and 6*s*-4*p* bands, where the observed transitions of the 4*p*-5*s* band were analyzed with a weight of ten times smaller than those for other bands.

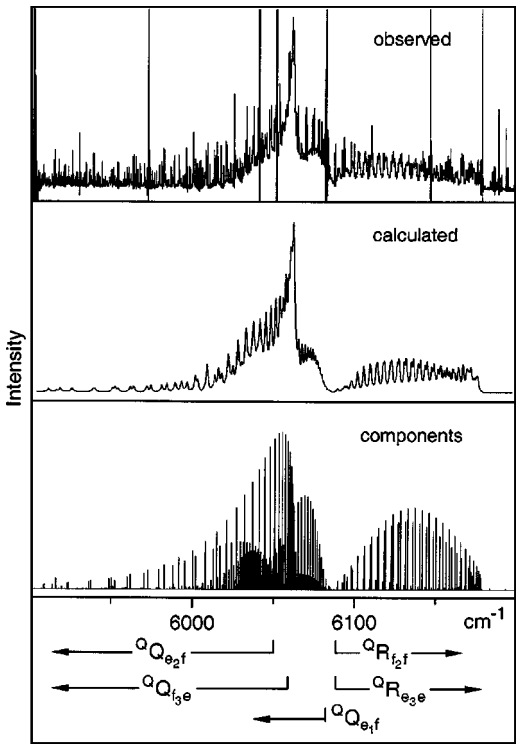

FIG. 1. Observed and calculated emission spectrum of the 4*p*-5*s* band of ArH. The strongest lines in the upper drawing originated from the Ar atom. Sharp lines belong to the 4*f*-3*d* band and probably to other unnassigned bands of ArH. To calculate the spectrum a ratio $|\mu_{\parallel}/\mu_{\perp}|=0.2$, $T=2500$ K, and a halfwidth of 0.7 cm^{-1} were assumed.

The bottom and middle parts of Fig. 1 show the calculated components and simulated contour of the band. The calculations were performed with $|\mu_{\parallel}/\mu_{\perp}|=0.2$, half linewidth of 0.7 cm^{-1}, and rotational temperature of $T=2500$ K (see below).

In our study we were able to observe spectra not only of the $v=0$-0 band but also for the vibrational sequence $v=1$-1, 2-2, 3-3, and probably 4-4 bands, as shown in Fig. 2. From the relative intensities of these bands a vibrational temperature of 2500 K was estimated. This temperature was used to simulate the bands under investigation. Moreover,

TABLE II. Assigned transitions in the $4p \rightarrow 5s$ $v=0$-0 band of ArH (in cm^{-1}). N'' is a quantum number N of the levels in the $5s$ state. In the notation for the line assignments, the left superscript indicates a value of R'-N'', the central letter defines a value of J'-J'', and the subscripts denote the components of the upper and lower states, respectively. The levels of given J and parity are labeled e_i and f_i in descending order of energy for p states and e and f for s states.

N''	${}^{Q}R_{e_3e}$		${}^{Q}R_{f_2f}$		${}^{Q}Q_{f_3e}$		${}^{Q}Q_{e_2f}$	
	Wave number	O–C	Wave number	O–C	Wave number	O–C	Wave number	O–C
8	6119.475	−0.166						
9	6124.004	−0.133	6118.728	0.082				
10	6128.534	−0.129	6123.098	0.088	6058.884	0.057		
11	6133.116	−0.080	6127.521	0.086	6057.316	0.027		
12	6137.752	0.045	6131.891	0.006	6055.415	−0.028		
13	6142.196	0.027	6136.367	0.044	6053.367	0.096		
14	6146.406	−0.142	6140.704	−0.007	6050.818	0.067		
15	6150.882	0.070	6145.074	0.064	6047.767	−0.092		
16	6155.038	0.113	6149.124	−0.056	6044.616	0.049		
17	6158.897	0.048	6153.120	−0.061	6040.813	−0.033		
18	6162.637	0.092	6156.945	−0.024	6036.676	0.012	6023.765	−0.045
19	6166.214	0.242	6160.509	0.008	6032.037	0.050		
20	6169.067	−0.019	6163.579	−0.153	6026.755	−0.024	6016.792	−0.011
21	6171.981	0.138			6020.904	−0.098	6012.368	−0.065
22					6014.619	0.002		
23	6176.040	−0.061			6007.515	−0.069	6001.646	0.107
24	6177.446	−0.059			5999.794	−0.065	5994.917	0.033
25					5991.353	−0.048	5987.390	0.035
26					5982.130	−0.034	5978.861	−0.055
27							5969.491	−0.043
28					5961.173	0.001	5959.151	−0.026
29					5949.248	−0.075	5947.806	−0.007
30					5936.523	0.013	5935.458	0.051
31					5922.716	0.032	5921.966	0.043
32					5907.817	0.020	5907.367	0.044
33					5891.827	0.027		
34					5874.693	0.048	5874.693	0.084
35					5856.294	0.012	5856.294	−0.115
36					5836.674	0.009		
37					5815.695	−0.048		

the differences in the band origin frequencies give a vibrational frequency for the $4p$ electronic state lower by 224 ± 5 cm^{-1} than that in the $5s$ state.

On the low-frequency side of the $v=1$-1 band one can see a partly resolved rotational structure consisting of lines having linewidths of 2–3 cm^{-1}. Analysis of this series has allowed the determination of some parameters of the first excited vibrational state. It was found that the observed lines belong to the most intense Q form branch ${}^{Q}Q_{f_3e}$ situated below the central peak, as shown in Fig. 2. We assigned well separated lines with N values from 20 to 34. The central peak in the lower part of Fig. 2 is explained by overlapping of low N transitions. To assign these lines, we estimated the vibration-rotation constant to be $\alpha(5s)=0.3738$ cm^{-1} for the $5s$ state of ArH by scaling from the ArD value.[2] Since there was no information on the vibrationaly excited states in the $4p$ state, α for the $4p$ state was assumed to be equal to that of the $5s$ state. It was also supposed that the band

TABLE III. Parameters of the 5s and 6s states of ArH (cm^{-1}). In Tables III–V the quoted uncertainties denote one standard deviation in units of the last digits.

	$5s$		$6s$	
Parameter	This work	Ref. 6	This work	Ref. 6
T			13 782.577(51)	13 782.502 6(25)
B	10.203 77(39)	10.204 1(38)	10.633 23(14)	10.632 40(18)
D 10^3	0.534 26(95)	0.562(21)	0.995 5(19)	0.964 0(27)
H 10^8	−0.582(27)	5.9(30)	49.1(11)	23.5(11)
L 10^{10}			−3.54(22)	
γ	0.081 2(26)	0.069 23[a]	0.025 36(42)	0.024 40(36)
γ_D 10^3	−0.034 4(36)		−0.022 46(28)	

[a]Estimated from ArD parameter.

TABLE IV. Parameters of the $4p$ and $5p$ states of ArH (cm^{-1}). Parameters in the square brackets were calculated for comparison from the parameters of Ref. 6 by expressions.

Parameter	$4p\sigma$	$4p\pi$	$5p\sigma$	$5p\pi$
		Diagonal		
T	6106.300(52) [6106.326] [a]	6069.982(51) [6069.992] [b]	17 550.792(51)	17 401.412(51)
B	10.442 89(34) [10.447 4] [c]	10.143 89(16) [10.140 6] [d]	10.462 57(26)	10.228 06(12)
$D\ 10^3$	0.629 4(20)	0.627 81(62)	0.679 5(31)	0.617 53(50)
$H\ 10^8$	−0.81(45)		3.4(11)	
γ	0.022 8(32)	−0.120 8(34)	−0.382 6(13)	
$\gamma_D\ 10^3$			0.108 8(92)	
$A^{\parallel}$		34.410 3(74) [34.587 8] [e]		11.160(37)
$A_D^{\parallel}\ 10^3$		−3.96(40)		0.057 04(88)
$A_H^{\parallel}\ 10^3$				−0.112 0(39)
$p\overline{L_+^2}$		−0.197 6(32)		
		Off-diagonal		
$A^{\perp}\overline{L_+}$	39.524 8(68) [39.729 3] [f]		21.274 2(94)	
$A_D^{\perp}\overline{L_+}\ 10^3$	−3.94(15)		−6.522(64)	
$\xi\overline{L_+}$	−24.108 0(15) [−24.570 9] [g]		−19.439 2(13)	
$\xi_D\overline{L_+}\ 10^3$	3.405(13)		4.956(19)	
$\xi_H\overline{L_+}\ 10^8$	27.2(48)		−44.8(80)	

[a] $T_\sigma = T + 2B - 2\xi - \frac{1}{2}\gamma - \frac{8}{3}G^{(2)} - \frac{4}{3}G_D^{(2)} - 4D + \frac{1}{2}A_D^{\perp}$.
[b] $T_\pi = T - \xi - \frac{1}{2}\gamma + \frac{1}{3}G^{(2)} + \frac{1}{4}A_D^{\perp}$.
[c] $B_\sigma = B - \frac{2}{3}G^{(2)} - 8D$.
[d] $B_\pi = B + \frac{1}{3}G^{(2)} - 2D$.
[e] $A^{\parallel} = A^{\parallel} + 4A_D^{\parallel} - \frac{1}{2}A_D^{\perp}$.
[f] $A^{\perp}\overline{L_+} = \sqrt{2}(2B - \xi - \gamma + A^{\perp} - \frac{4}{3}G_D^{(2)} - 8D + 2A_D^{\perp})$.
[g] $\xi\overline{L_+} = \sqrt{2}(-2B + \xi + \frac{4}{3}G_D^{(2)} + 8D)$.

origins $4p\sigma \rightarrow 5s$ and $4p\pi \rightarrow 5s$ $v = 1\text{-}1$ were those for $v = 0\text{-}0$ decreased by 224 cm^{-1}. Corresponding values were $T_1(4p\sigma) = 5882.300$, $T_1(4p\pi) = 5845.982$, $B_1(5s) = 9.830$, $B_1(4p\sigma) = 10.0691$, and $B_1(4p\pi) = 9.7701$ cm^{-1}. All other parameters were assumed to be same as those of the $v = 0$ states. Only two constants $T_1(4p\pi)$ and $B_1(4p\pi)$ were varied during the fitting and determined to be $T_1(4p\pi) = 5845.77 \pm 0.28$ cm^{-1} and $B_1(4p\pi) = 9.773\ 26 \pm 0.000\ 35$ cm^{-1} which are close to the initial ones. Assigned transitions are listed in Table V.

It was found that linewidths of the best resolved and most intense series ${}^{Q}Q_{f_3 e}$ of the 0-0 band decrease with increasing rotational quantum number (see Fig. 3). The observed widths were in the range of 0.38–1.2 cm^{-1}. Similar rotational dependence of linewidths has been reported for various diatomic molecules such as OH,[12] OD,[13] N_2^+,[14] CO,[15] NaK,[16] Li_2,[17] and was detected in one of the rare gas hydrides, HeH.[18] In our case the observed effect is caused by homogeneous predissociation of the $5s(A\,{}^2\Sigma^+)$ state by the repulsive ground state $4s(X\,{}^2\Sigma^+)$ as has been reported for HeH.[18] The ground repulsive electronic state $X\,{}^2\Sigma^+$ and bound $A\,{}^2\Sigma^+$ state are coupled by the radial matrix elements which were calculated in several papers at different levels of accuracy.[19–22] Homogeneous interaction obeys the selection rules $\Delta J = 0$, $\Delta\Lambda = 0$, $\Delta S = 0$, $\Delta\Sigma = 0$, and $+ \leftarrow | \rightarrow -$.

We simulated the observed phenomena following the theory described in Refs. 19 and 20 and using the potential curves of the states under consideration and radial coupling elements given in Figs. 1 and 2 of the paper by Petsalakis and Theodorakopoulos.[21] The simulations are reproduced in Fig. 4. Widths of the energy levels predissociated by the continuum of the neighboring repulsive state were calculated by the Fermi's golden rule formula

$$\Gamma = 2\pi |\langle \chi_{E,j} | T_N | \chi_{v,j} \rangle|^2, \tag{11}$$

where $\chi_{v,j}$ and $\chi_{E,j}$ are nuclear functions of the $A\,{}^2\Sigma^+$ and $X\,{}^2\Sigma^+$ electronic states, both having equal energies. $\chi_{v,j}$ and $\chi_{E,j}$ should be, respectively, unit and energy normalized. T_N is defined (in atomic units) by the expression

$$T_N = -\frac{1}{2\mu}\left\{ B(R) + 2A(R)\frac{\partial}{\partial R} \right\}. \tag{12}$$

$A(R)$ and $B(R)$ are matrix elements of the first and second derivatives over two electronic states Ψ_{el}^X and Ψ_{el}^A,

$$A(R) = \left\langle \Psi_{el}^X \left| \frac{\partial}{\partial R} \right| \Psi_{el}^A \right\rangle, \quad B(R) = \left\langle \Psi_{el}^X \left| \frac{\partial^2}{\partial^2 R} \right| \Psi_{el}^A \right\rangle. \tag{13}$$

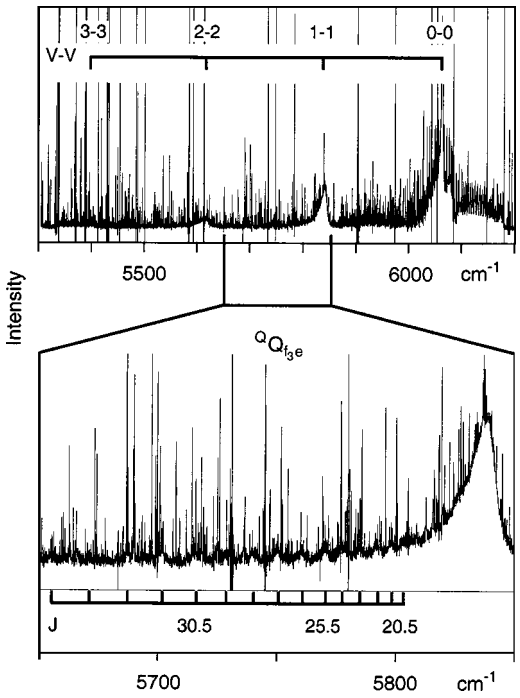

FIG. 2. Observed 4*p*-5*s* transitions between vibrationally excited levels.

The bound and continuum nuclear wave functions $\chi_{v,j}$ and $\chi_{E,j}$ have been obtained by numerical diagonalization of the matrix of the Hamiltonian operator

$$H = -\frac{\hbar^2}{2\mu}\frac{d^2}{dR^2} + \left(V(R) + \frac{\hbar^2}{2\mu R^2}J(J+1)\right) \tag{14}$$

expanded by a set of orthonormal basis functions,

$$\sqrt{\frac{2}{R_U - R_L}}\sin\left(\frac{\pi n(R - R_L)}{R_U - R_L}\right), \quad n = 1,2,3,\cdots, \tag{15}$$

where R is an internuclear separation, and R_U and R_L are the upper and lower integration limits. The limited integration range is equivalent to the inclusion of two steep walls to the potential in the R_U and R_L positions. R_L has to be placed in

TABLE V. Assigned transitions in the $^{Q}Q_{f_3e}$ branch of the 4*p*-5*s* $v=1$-1 band of ArH (cm^{-1}). N'' is a quantum number N of the levels in the 5*s* state.

N''	Wave number	O–C
20	5803.03	−0.61
21	5798.22	0.19
22	5791.98	0.18
23	5784.65	−0.27
24	5777.17	−0.19
25	5769.45	0.37
26	5760.20	0.19
27	5750.19	0.06
28	5739.53	0.14
29	5728.16	0.43
30	5715.30	0.19
31	5701.11	−0.37
32	5686.94	0.13
33	5670.63	−0.39
34	5654.00	−0.08

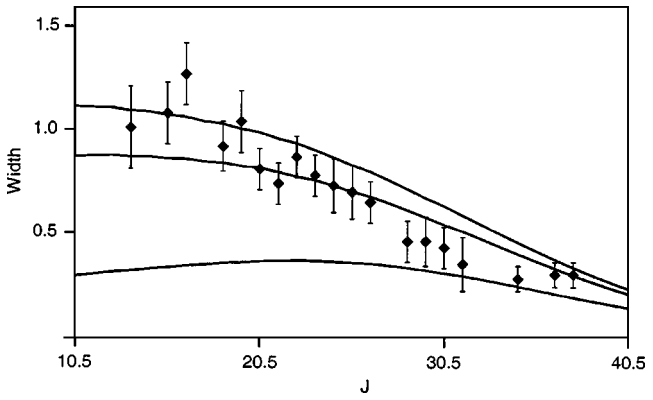

FIG. 3. Decreasing of the linewidth in the $^{Q}Q_{f_3e}$ form branch of the 4*p*-5*s* transition of ArH. The changing parameter of the calculated curves is a shift of the repulsive potential curve with respect to the bound potential curve in angstroms.

the classical forbidden region where actual wave functions are asymptotically equal to zero. R_U has a large value of the internuclear distance where bound vibrational functions have also negligibly small values, and where the continuum wave functions $\chi_{E,j}$ correspond to the case of a dissociated molecule. It should be noted that the basis functions given in Eq. (15) differ from those used by Petsalakis, Theodorakopoulos, and Buenker,[19] where they were not reduced to zero at the bounding walls. The walls do not affect the bound vibrational functions but transform continuum wave functions into a quasicontinuum. The energies of the (E,j) and (v,j) states must coincide when calculating the width Γ. Therefore, after computing the rotation-vibrational energies of the bound states, the position of the far wall was varied near R_U to obtain the same energy for one of the quasicontinuum levels. The nuclear functions obtained in this way were employed to evaluate widths Γ.

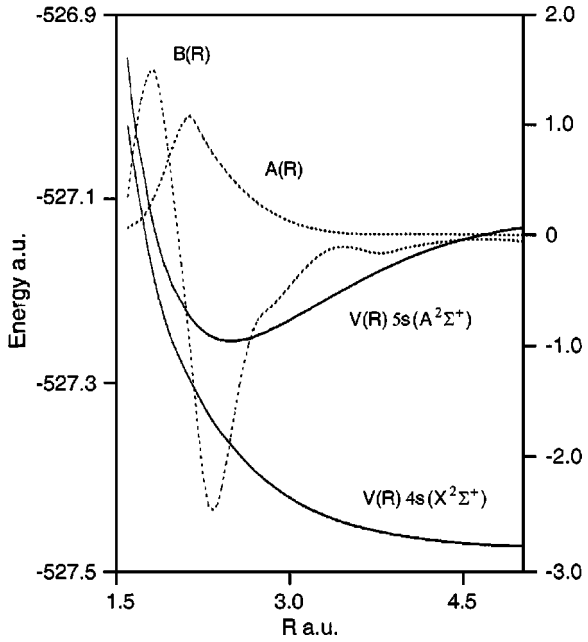

FIG. 4. *Ab initio* potential curves and A and B coupling matrix elements from Ref. 21.

TABLE VI. Linewidths of ArH and ArD in the 4*p*-5*s* band for low $J(\mathrm{cm}^{-1})$.

	v	Observed[a]	Shift[b] =0			0.007	0.009
			Ref. 21	Ref. 22	This work	This work	
ArH	0	1.2	0.19	0.367	0.245	0.862	1.128
	1	~(2–2.4)	0.64	0.930	0.389	2.146	2.967
ArD	0	<0.05	0.01	0.014	0.025	0.008	0.004
	1	~0.1	0.04	0.079	0.177	0.075	0.048

[a]Observed widths for ArH are from the present work, for ArD they are taken from Ref. 2.
[b]Shifts of the repulsive state potential curve with respect to potential curve of the bound 5*s* state are in angstroms.

To check our program we have calculated matrix elements of $B(R)$ over functions $\chi_{v,j}$ and $\chi_{E,j}$ using Le Roy's "BCONT 2.2" predissociation computer code obtained from the http://leroy.uwaterloo.ca website. The results of these calculations were similar to ours. However, Le Roy's code does not allow for a partial derivative coupling function operator, so we could not make a comparison of matrix elements containing $A(R)$. Also, two independent procedures have been applied for the energy normalization of the quasicontinuum functions $\chi_{E,j}$.

The first one employed the interpolation formula[19]

$$\tilde{\Gamma}_k = \frac{2\Gamma_k}{\varepsilon_{k-1} + \varepsilon_{k+1}}, \tag{16}$$

where ε_k is an eigenvalue corresponding to the kth function $\chi_{E,j}$ and $\tilde{\Gamma}_k$ stands for the energy-normalized quantity of the width, whereas Γ_k is calculated with the unit normalized $\chi_{E,j}$ for kth energy level. According to the second method,[23] Γ_k was calculated with unit asymptotic normalization of the quasicontinuum wave function $\chi_{E,j}$ and applying correction factor $\sqrt{8\mu/h^2[\varepsilon_k - V(R=\infty)]}$. Both methods gave the same results.

Since analytic expressions for $V(R)$, $A(R)$, $B(R)$ or their numerical values were not available, the curves of these functions presented in Fig. 4 were manually digitized and in this form used in calculations. The results obtained are given in Table IV and Fig. 3. A basis set of 118 functions given by Eq. (15) with $R_L = 1.6$ and $R_U = 9.5$ a.u. was utilized. It should be noted that a more accurate plot for $A(R)$ was shown in Ref. 22. However, for our aim of a qualitative description it was sufficient to use the more smooth $A(R)$ from Ref. 21 which could be digitized with higher accuracy. Table VI contains measured and calculated linewidths for small J values of the ArH and ArD isotopes in the two lowest vibrational states, where the linewidths of ArH in the $v=0$, 1 states as measured in the present study are listed. Although the same $V(R)$, $A(R)$, and $B(R)$ values were used the presently calculated widths do not coincide exactly with those obtained in the original study.[21] This is presumably due to errors in data transformation from graphical to digital and due to the fact that the results are very sensitive to such small differences. Roche and Tellinghuisen[14] and Hemert, Dohmann, and Peyerimhoff[20] noted that calculated predissociation rates are extremely sensitive to small variations in the relative positions of the potential curves of the electronic states. We have calculated the linewidths for different shifts of the repulsive state potential function with respect to the bound state potential curve and have found that the shifts in the region of 0.007–0.009 Å reproduce the experimental values both for ArH and ArD (Table VI, Fig. 3). This indicates that a relatively small improvement of the *ab initio* values of $V(R)$, $A(R)$, and $B(R)$ could lead to a better agreement between observed and calculated values of the predissociation rate.

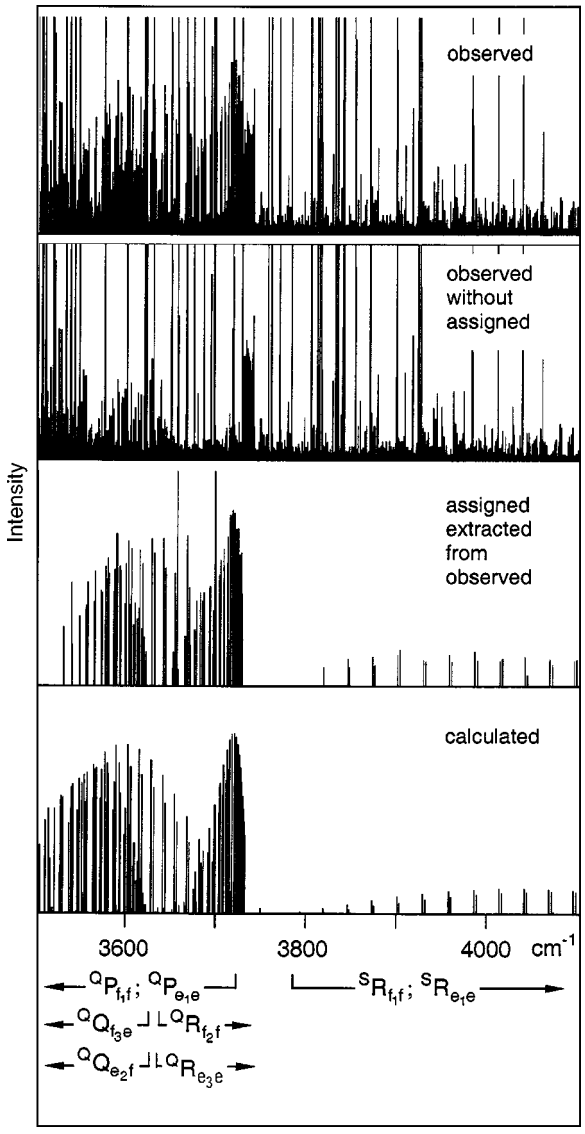

FIG. 5. Observed and calculated emission spectrum of the 5*p*-6*s* band of ArH. To simulate spectrum it was assumed $|\mu_\parallel/\mu_\perp| = 0.9$ and $T = 2500$ K.

TABLE VII. Assigned transitions in the $5p \rightarrow 6s$ band of ArH (in cm^{-1}). N'' is a quantum number N of the levels in the 6*s* state.

N''	$^{S}R_{f_1f}$		$^{S}R_{e_1e}$		$^{Q}P_{e_1e}$		$^{Q}P_{f_1f}$			
	Wave number	O–C	Wave number	O–C	Wave number	O–C	Wave number	O–C	Wave number	O–C
0			3791.176	0.002						
1	3817.439	0.003	3816.188	−0.002						
2	3844.307	0.008	3842.634	−0.001			3728.207	0.002		
3	3872.073	0.005	3870.043	−0.002	3709.963	−0.008	3711.273	0.005		
4	3900.352	0.002	3898.019	−0.003	3694.102	−0.002	3695.820	0.003		
5	3928.847	0.003	3926.257	0.001	3679.360	−0.004	3681.439	0.005		
6	3957.326	−0.003	3954.526	0.000	3665.385	−0.009	3667.771	0.002		
7	3985.644	−0.005	3982.676	0.001	3651.928	0.002	3654.548	−0.010		
8	4013.691	−0.006	4010.597	0.001	3638.779	0.005	3641.619	−0.001		
9	4041.392	−0.003	4038.219	−0.001	3625.820	0.005	3628.829	−0.001		
10	4068.686	−0.002	4065.503	−0.001	3612.976	0.004	3616.108	−0.003		
11	4095.537	0.000	4092.422	−0.004	3600.204	0.002	3603.410	−0.002		
12					3587.487	0.000	3590.707	0.002		
13					3574.831	0.001	3577.980	0.010		
N''	$^{Q}R_{f_2f}$		$^{Q}R_{e_3e}$		$^{Q}Q_{f_3e}$		$^{Q}Q_{e_2f}$		$^{Q}P_{e_2e}$	
0			3639.077	−0.002						
1	3649.560	−0.003	3653.330	−0.010	3619.981	0.005				
2	3662.645	−0.001	3665.385	0.010	3617.628	0.002				
3	3673.233	−0.003	3675.393	−0.010	3614.891	0.004	3612.480	0.002		
4	3681.992	0.000	3683.757	−0.011	3611.535	0.002	3609.671	0.020		
5	3689.317	−0.002	3690.769	−0.010	3607.525	0.003	3605.945	−0.005		
6	3695.500	−0.005	3696.678	−0.010	3602.868	0.005	3601.477	−0.007		
7	3700.770	0.005	3701.690	−0.004	3597.586	0.003	3596.317	−0.006		
8	3705.277	0.009	3705.959	0.001	3591.732	0.013	3590.515	−0.009		
9	3709.157	0.010	3709.613	0.006	3585.324	0.010	3584.126	−0.009		
10	3712.517	0.010	3712.756	0.007	3578.436	0.026	3577.193	−0.007		
11	3715.422	−0.017	3715.490	0.020	3571.055	0.005	3569.748	−0.009	3569.477	−0.022
12	3718.012	−0.002	3717.848	0.005	3563.268	−0.005	3561.831	−0.002	3561.553	−0.007
13	3720.285	−0.006	3719.925	−0.002	3555.106	−0.010	3553.452	0.004	3553.165	0.004
14	3722.310	−0.009	3721.766	−0.006	3546.602	−0.009	3544.616	0.014	3544.319	0.016
15	3724.133	−0.007	3723.410	−0.008	3537.778	−0.011	3535.292	0.012	3534.975	0.005
16	3725.805	0.016	3724.902	0.001	3528.685	0.010	3525.416	−0.020		

B. 5*p*-6*s* band

This band is observed around 3700 cm^{-1}. It was observed previously for both ArH and ArD,[5] but was analyzed only for ArD because the 5*p*-6*s* band of ArH appears in a congested region that is difficult to analyze without further information. An overall view of the part of the spectra containing this band is presented in Fig. 5.

The rotation-electronic lines were assigned by straightforward calculation of transition wave numbers using parameters of the 6*s* and 5*p* states. The constants of the 6*s* state were taken from Ref. 6, whereas the parameters of the 5*p* state were obtained by isotope scaling of the ArD constants in accordance with the known isotope relations: $B \sim \mu^{-1}, D \sim \mu^{-2}, A^{II} \sim \mu^{0}, A^{\perp} \sim \mu^{0}, \xi \sim \mu^{-1}, \gamma \sim \mu^{-1}, p \sim \mu^{-1}$, where μ is the reduced molecular mass. Since the available parameters correspond to those of the effective Hamiltonian of *l* complexes and since we used a different form of the Hamiltonian, we preliminarily calculated rotational levels of the electronic states under consideration with the Hamiltonian of *l* complexes, and then the initial values of the constants of the Hamiltonian expressed by relations (6) and (8) were derived from these levels. As in the case of ArD it was found that the most intense part of the 5*p*-6*s* band of ArH was formed by couples of $^{Q}P_{e_1e}$ and $^{Q}P_{f_1f}$-, $^{Q}Q_{e_2f}$- and $^{Q}Q_{f_3e}$-, $^{Q}R_{f_2f}$-and $^{Q}R_{e_3e}$ form branches. Also just as for the ArD band, the *S* branches were found as doublets in the high-frequency end of the ArH band. In the middle of Fig. 5, an investigated part of the spectrum is divided into two parts. One of them contains only the assigned lines among observed transitions and the other part shows observed spectra without assigned transitions. In the central part of the spectra with removed assigned lines one can see a congested group near 3730 cm^{-1} which belongs to the $^{Q}R_{f_2f}$- and $^{Q}R_{e_3e}$ form branches. The lines with $N > 16$ are perturbed and could therefore not be assigned. In the bottom of Fig. 5 the simulated 5*p*-6*s* band is presented which has been calculated under the assumptions $T = 2500$ K and $|\mu_{\parallel}/\mu_{\perp}| = 0.9$ and the *N* value up to 16 which is the largest value identified in the present study. In Ref. 5 the rotational energy levels of the 4*p*, 5*p*, and 6*p* states of ArD were analyzed. It was noted that e_1 and e_2 levels of the 5*p* state of ArD are affected by the avoided crossing in the rotational levels with $N > 25$. The present results indicate that the crossing of these levels of the 5*p* state of ArH occurs for $N = 17$. Other *e* and *f* levels do not

TABLE VIII. Assigned transitions in the $6s \rightarrow 4p$ band of ArH (in cm^{-1}). N' is a quantum number N of the levels in the $6s$ state. Asterisks mark new assignments.

N'	$^{O}P_{ff_1}$		$^{Q}R_{ff_1}$		$^{Q}P_{ff_2}$		$^{S}R_{ff_2}$		$^{Q}P_{ff_3}$	
	Wave number	O–C	Wave number	O–C	Wave number	O–C	Wave number	O–C	Wave number	O–C
0	7604.238	−0.002			7693.530	−0.007				
1	7568.142	−0.016	7704.424	0.002	7692.470	−0.007			7724.069	−0.011
2	7532.693	0.017	7710.399	−0.010	7692.018	−0.002	7799.707	0.002	7725.815	0.010
3	7497.882	0.017	7716.641	0.001	7692.093	−0.004	7840.961	0.002	7728.622	−0.005
4	7463.745	−0.005	7723.312	0.003	7692.674	0.003	7882.661	0.007	7732.474	−0.023
5	7430.330	−0.003	7730.451	0.005	7693.717	0.000	7924.683	0.005	7737.366	0.010
6	7397.606	−0.001	7738.032	−0.003	7695.208	−0.001	7966.961	0.005	7743.139	−0.005
7	7365.566	0.007	7746.038	−0.004	7697.114	−0.008			7749.780*	−0.20
8	7334.179	0.003	7754.425	−0.001	7699.426	−0.006			7757.273*	0.009
9	7303.435*	−0.007	7763.147	0.002	7702.101	−0.008				
10	7273.332*	−0.013	7772.163	0.005	7705.122*	−0.006				
11	7243.901*	0.025	7781.425	0.000	7708.460*	−0.003				
12			7790.891	−0.020	7712.094*	0.001				
14					7720.169*	0.010				

N'	$^{Q}Q_{fe_1}$		$^{Q}Q_{fe_2}$		$^{Q}Q_{ef_3}$		$^{O}P_{ee_1}$		$^{Q}R_{ee_1}$	
1	7700.872	−0.015					7637.160	−0.001		
2	7705.250	0.001	7734.120*	0.009	7723.546	0.007	7599.109	−0.008	7695.863	0.003
3	7710.065	0.003	7739.628*	0.018	7724.149	0.006	7561.643	−0.001	7700.955	0.005
4	7715.500	0.003			7725.904	0.011	7524.953	0.001	7705.339	0.003
5	7721.586	−0.006	7752.415*	−0.001	7728.728	−0.011	7489.123	0.000	7710.177	0.003
6	7728.345	−0.002			7732.632	0.000	7454.199	0.002	7715.632	−0.001
7	7735.733	−0.010			7737.520	0.005	7420.190	−0.002	7721.752	0.001
8	7743.762	0.011	7775.878*	−0.013	7743.320	−0.005	7387.118*	0.006	7728.536	0.009
9	7752.333*	−0.003	7784.671*	0.012	7749.993	−0.009	7354.959*	0.007	7735.948	0.004
10	7761.471*	0.011	7793.817*	−0.004	7757.492	0.006	7323.700*	0.001	7743.968	−0.004
11	7771.076*	−0.005	7803.345*	0.001	7765.734	0.015			7752.574	−0.002
12	7781.147*	−0.011							7761.716	−0.001
13									7771.351*	−0.003

N'	$^{O}P_{ee_2}$		$^{Q}R_{ee_2}$		$^{Q}P_{ee_3}$		$^{S}R_{ee_3}$	
1	7665.031	0.005						
2	7627.980	0.000			7693.375	−0.004		
3	7591.186	−0.005	7728.818	0.004	7690.888	−0.008		
4	7555.159	0.003	7734.206	0.007	7689.324	−0.004		
5	7519.945	−0.002	7739.722	0.000	7688.509	0.002	7839.426	0.000
6	7485.565	−0.005	7745.838	0.001	7688.355	−0.001	7880.016	0.007
7	7452.008	−0.004	7752.574	−0.001	7688.817	−0.001	7921.141	0.006
8	7419.252	0.000	7759.895	−0.005	7689.844	−0.002	7962.688	0.002
9	7387.270	−0.004	7767.759	−0.004	7691.392	−0.003	8004.575*	0.005
10	7356.065	0.004	7776.101	−0.012	7693.417*	−0.005		
11	7325.589	−0.012	7784.899	0.000	7695.879*	−0.005		
12	7295.901*	0.011	7794.081	0.002	7698.750*	0.006		
13	7266.937*	0.004	7803.624*	0.007	7701.972*	0.005		
14	7238.745*	0.000	7813.494*	0.008	7705.538*	0.015		
15	7211.333*	−0.020	7823.672*	0.003	7709.410*	0.023		
16			7834.145*	−0.013	7713.505*	−0.032		
17			7844.976*	0.020				

cross. So the above mentioned perturbation in the $5p$-$6s$ band of ArH arises from an interaction with another electronic state. All assigned transitions are listed in Table VII while the constants are listed in Table IV.

As was noted, in order to determine the rotational energy values of electronic states connected with the lowest $5s$ level we carried out a combined fitting including not only the $4p$-$5s$ and $5p$-$6s$ bands, but also the $6s$-$4p$ band. The $6s$-$4p$ band in the 7700 cm^{-1} region was previously studied by Dabrowski, Tokaryk, and Watson,[6] and in the present study transitions with larger rotational states have been observed and analyzed. All transitions used in the least-squares analysis are given in Table VIII where the lines labeled with asterisks have been measured and assigned for the first time.

V. CONCLUSIONS

An infrared emission spectrum of ArH by a dc discharge in an argon-hydrogen mixture was observed. The $4p$-$5s$ band in the 6100 cm^{-1} region and the $5p$-$6s$ band in the 3700 cm^{-1} region were analyzed by using the N^2 formulation for energy levels. A linewidth dependence on the rotational quantum number N was observed for the $4p$-$5s$ band together with linewidth broadening for transitions originating from vibrationally excited states. The parameters obtained here are presented in a nontraditional manner but they can be transformed to the set of parameters of other commonly accepted Hamiltonians. There are still many unassigned bands in the observed spectra including higher vibrationally excited v-v bands. Some of them will be analyzed in the near future.

ACKNOWLEDGMENTS

The authors are deeply grateful to J. K. G. Watson for supplying the file of all assigned transitions of ArH and ArD used in the previous studies (Refs. 4–8) and also wish to thank G. Theodorakopoulos for valuable discussions. The authors acknowledge Robert Le Roy for free access to the code of his BCONT program.

[1]H. H. Michels and F. E. Harris, J. Chem. Phys. **39**, 1464 (1963).
[2]J. W. C. Johns, J. Mol. Spectrosc. **36**, 488 (1970).
[3]R. H. Lipson, Mol. Phys. **65**, 1217 (1988).
[4]I. Dabrowski, G. DiLonardo, G. Herzberg, J. W. C. Johns, D. A. Sadovskii, and M. Vervloet, J. Chem. Phys. **97**, 7093 (1992).
[5]I. Dabrowski, D. W. Tokaryk, M. Vervloet, and J. K. G. Watson, J. Chem. Phys. **104**, 8245 (1996).
[6]I. Dabrowski, D. W. Tokaryk, and J. K. G. Watson, J. Mol. Spectrosc. **189**, 95 (1998).
[7]I. Dabrowski, D. W. Tokaryk, R. H. Lipson, and J. K. G. Watson, J. Mol. Spectrosc. **189**, 110 (1998).
[8]C. R. Nowlan, D. W. Tokaryk, and J. K. G. Watson, Can. J. Phys. **79**, 189 (2001).
[9]R. N. Zare, A. L. Schmeltekopf, W. J. Harrop, and D. L. Albritton, J. Mol. Spectrosc. **46**, 37 (1973).
[10]J. M. Brown, E. A. Colbourn, J. K. G. Watson, and F. D. Wayne, J. Mol. Spectrosc. **74**, 294 (1979).
[11]J. T. Hougen, *The Calculation of Rotational Energy Levels and Rotational Line Intensities in Diatomic Molecules* (U.S. Government Printing Office, Washington, DC, 1970).
[12]A. G. Gaydon and H. G. Wolfhard, Proc. R. Soc. London, Ser. A **208**, 63 (1951).
[13]J. Czarny, P. Felenbok, and H. Lefebvre-Brion, J. Phys. B **4**, 124 (1971).
[14]A. L. Roche and J. Tellinghuisen, Mol. Phys. **38**, 129 (1979).
[15]J. Baker, W.-U. L. Tchang-Brillet, and P. S. Julienne, J. Chem. Phys. **102**, 3956 (1995).
[16]Z. J. Jabboura and J. Huennekens, J. Chem. Phys. **107**, 1094 (1997).
[17]S. Antonova, G. Lazarov, K. Urbanski, A. M. Lyyra, L. Li, G.-H. Jeung, and W. C. Stwalley, J. Chem. Phys. **112**, 7080 (2002).
[18]W. Ketterle, A. Dodhy, and H. Walter, J. Chem. Phys. **89**, 3442 (1988).
[19]I. D. Petsalakis, G. Theodorakopoulos, and R. J. Buenker, J. Chem. Phys. **92**, 4920 (1990).
[20]M. C. van Hemert, H. Dohmann, and S. D. Peyerimhoff, Chem. Phys. **110**, 55 (1986).
[21]I. D. Petsalakis and G. Theodorakopoulos, J. Phys. B **25**, 5353 (1992).
[22]G. Theodorakopoulos and I. D. Petsalakis, J. Chem. Phys. **101**, 194 (1994).
[23]J. N. Murrell and J. M. Taylor, Mol. Phys. **16**, 609 (1969).